Available online at www.sciencedirect.com
SCIENCE DIRECT®
Journal of Sound and Vibration 266 (2003) 107–117
JOURNAL OF SOUND AND VIBRATION
www.elsevier.com/locate/jsvi

# Study of second-harmonic generation of shear horizontal modes using modal analysis

Ming-Xi Deng*

*Department of Physics, Logistics Engineering University, No. 174, Chang Jiang 2 Road, Chongqing 400016, People's Republic of China*

Received 22 April 2002; accepted 21 November 2002

**Abstract**

In this work a modal analysis was employed to study generation of the second harmonics of shear horizontal (SH) modes in a solid plate. Under second order perturbation, second-harmonic generation will occur accompanying SH mode propagation due to the bulk elastic non-linearity of plate material. In solid plate the total second-harmonic fields of a SH mode propagation are regarded as sum of the fields of a series of double frequency Lamb modes (DFLMs). The contribution of each DFLM component to the total second-harmonic fields is dependent of the difference of phase velocities of the corresponding DFLM and SH mode. The analysis results show that the DFLM field component may have cumulative growth effect once its phase velocity exactly or approximately equals that of a SH mode. It is also found that the fields of the total second harmonics of a SH mode are only symmetrical. The examples of field distributions of several DFLMs on the plate surface are considered.


## 1. Introduction

The propagation of guided wave modes such as Lamb modes and shear horizontal (SH) modes is well understood and encountered in many practical situations [1,2]. In general, each guided wave mode can be though of as superposition of partial bulk acoustic waves satisfying the corresponding boundary conditions. The characteristics of guided wave modes can be used in the non-destructive evaluation of plate materials [3]. Recently, it is being realized that the linear characteristics of guided wave modes are often not sufficient. The non-linear elasticity of engineering materials may be a very sensitive indicator of some defect states that are difficult to

*Fax: +86-23-68590915.
*E-mail address:* hgwldmx@cta.cq.cn (M.-X. Deng).

0022-460X/03/$ - see front matter © 2003 Elsevier Ltd. All rights reserved.
doi:10.1016/S0022-460X(02)01578-X

detect by other means [4,5]. Thus, the non-linear effect of guided wave modes is evoked, necessitating a non-linear analysis of guided wave modes.

Generally, the non-linear problem of a guided wave mode is very difficult to solve. However, often the elastic non-linearity is small and a perturbation approach can be applicable [6]. Whereas a SH mode is one of the simplest guided wave modes, investigation of the non-linear effect of SH modes will lay a foundation for studying that of the other guided wave modes. For simplicity, in this article, all analyses are performed for SH modes, and second order perturbation is applied, and only the elastic non-linearity is considered. Under second order perturbation, generation of the second harmonics will occur as SH modes propagate in the solid plate. In general, the dispersive nature of SH modes ensures that there is no strong non-linear effect. Thus, it is difficult to use the dynamic non-linear elasticity of SH modes of a solid plate for its characterization.

Theoretical analysis of second-harmonic generation with a cumulative growth effect was reported in the literature by Deng [7]. It is found that there is a strong non-linear effect once the phase velocity of a SH mode propagation equals the longitudinal velocity of the plate material, and that the corresponding fields of the second harmonics are symmetrical. In that theoretical study the analysis method used to investigate the problems of non-linear acoustic reflection at an interface is applied [8]. Although some primary interesting results have been obtained, there are still problems to be solved such as that non-cumulative second-harmonic terms cannot be determined. Thus, the further analysis is needed.

Second order perturbation reduces a complicated non-linear problem to the linear one with known sources, so that linear analysis techniques can be employed even if the original problem is non-linear. It is well known that the modal analysis offering an effective approach for treating the problem of waveguide excitation is widely applied in acoustics [2,9–11]. The principle of a modal analysis is to express the excited fields as superposition of normal modes obtained in a stress-free waveguide. The contribution of each normal mode component is determined by the corresponding excitation source distribution. To the author's knowledge, no effort to date has been paid on the analysis of second-harmonic generation of guided wave modes using a modal analysis.

In this paper the modal analysis of waveguide excitation is employed to study second-harmonic generation of SH modes under second order perturbation. The analysis process shows a clear insight into physical process of second-harmonic generation of SH modes, and the solution obtained overcomes the shortcoming of the previous results that non-cumulative second-harmonic terms cannot be determined.

## 2. General considerations

Under second order perturbation the motion equations governing the fundamental frequency (primary) and double frequency waves of a solid are given by [6,12]

$$\rho\frac{\partial^2\mathbf{u}^{(1)}}{\partial t^2} - (\kappa + 4\mu/3)\nabla(\nabla\cdot\mathbf{u}^{(1)}) + \mu\nabla\times(\nabla\times\mathbf{u}^{(1)}) = 0,$$
$$\rho\frac{\partial^2\mathbf{u}^{(2)}}{\partial t^2} - (\kappa + 4\mu/3)\nabla(\nabla\cdot\mathbf{u}^{(2)}) + \mu\nabla\times(\nabla\times\mathrm{u}^{(2)}) = \mathbf{F}(\mathbf{u}^{(1)}), \quad (1)$$

where $\mathbf{u}^{(1)}$ and $\mathbf{u}^{(2)}$ denote the fundamental frequency and the double frequency displacements, respectively; $\rho$, $\kappa$ and $\mu$ are mass density and second order elastic constants of the solid. We assume that the material of a solid plate is isotropic and lossless, and that the position of excitation source of SH modes is located at $z = 0$, and that only the $m$th SH mode with angular frequency $\omega$ is generated in the plate of thickness $2d$ (Fig. 1). The solution to the $m$th SH mode satisfying the first of Eq. (1) takes the form [2,7]

$$\mathbf{u}_{(m)Ti} = u_{(m)Ti}\hat{x}\exp[\mathrm{j}\mathbf{K}_{(m)Ti}\cdot\mathbf{r} - \mathrm{j}\omega t], \quad i = 1, 2 \tag{2}$$

with

$$\mathbf{K}_{(m)Ti}\cdot\mathbf{r} = k_{(m)}z + (-1)^{\mathrm{i}-1}\alpha_{(m)}k_{(m)}y, \quad \left|\mathbf{K}_{(m)Ti}\right| = K_T = \omega/c_T,$$
$$k_{(m)} = K_T\sin\theta_{(m)T}, \quad \cos\theta_{(m)T} = \alpha_{(m)T}\sin\theta_{(m)T}, \quad \alpha_{(m)T} = \sqrt{\left[c_{(m)}^2/c_T^2\right] - 1}, \tag{3}$$

where the subscript '$m$' denotes the ordinal number of a SH mode, $c_T$ is the transverse velocity of plate material, $k_{(m)} = \omega/c_{(m)}$ is the $oz$-axis component of $\mathbf{K}_{(m)T1}$ and $\mathbf{K}_{(m)T2}$, $c_{(m)}$ is the phase velocity of the $m$th SH mode whose existence is postulated, and the other physical quantities are shown in Fig. 1. Here and below a physical quantity with '^' means an unit vector of the corresponding quantity. The displacement component along the $ox$-axis is written as

$$u_x^{(1)} = u_{(m)T1}\exp[\mathrm{j}\mathbf{K}_{(m)T1}\cdot\mathbf{r} - \mathrm{j}\omega t] + u_{(m)T2}\exp[\mathrm{j}\mathbf{K}_{(m)T2}\cdot\mathbf{r} - \mathrm{j}\omega t]. \tag{4}$$

The phase velocity of the $m$th SH mode determined by the boundary condition (stress tensor component at $y = \pm d$ is zero, i.e., $\partial u_x^{(1)}/\partial y|_{y=\pm d} = 0$) is given by [2,7]

$$c_{(m)} = \frac{c_T}{\sqrt{1 - \left(mc_T/4fd\right)^2}}, \tag{5}$$

where $f$ is the excitation frequency, and $fd$ is the product of frequency and half of plate thickness. There is a relation between $u_{(m)T1}$ and $u_{(m)T2}$, i.e., $u_{(m)T1} = (-1)^m u_{(m)T2}$.

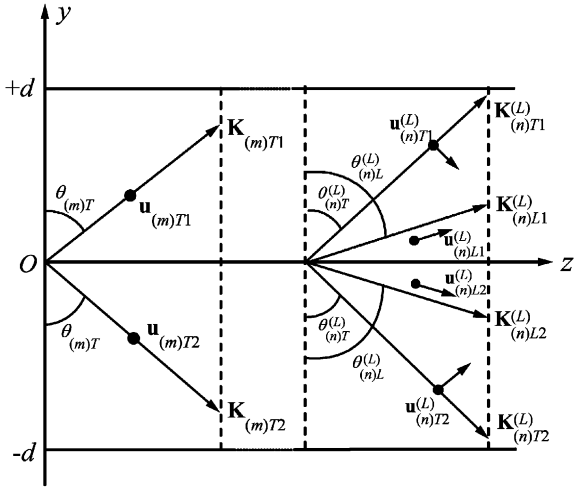


Fig. 1. Acoustic fields of the $m$th SH mode and the $n$th DFLM.

Considering a single SH mode with ordinal number $m$ propagating in a solid plate, under second order perturbation, there is a bulk driving force of double frequency in the plate due to the bulk elastic non-linearity of the plate material (i.e., $\mathbf{F}(\mathbf{u}^{(1)})$ in the second of Eq. (1)). This bulk driving force may be regarded as the source of waveguide excitation.

For the $m$th SH mode the fundamental frequency displacement field in the plate is $\mathbf{u}^{(1)} = \mathbf{u}_{(m)T1} + \mathbf{u}_{(m)T2} = u_x^{(1)}\hat{x}$. The driving force in the plate due to the bulk elastic non-linearity is found to be [omitting the factor $\exp(-\mathrm{j}2\omega t)$] [7,12]:

$$\begin{aligned}
&\mathbf{F}(\mathbf{u}^{(1)}) = F_{(m)Ti}\hat{\mathbf{K}}_{(m)Ti}\exp(\mathrm{j}2\mathbf{K}_{(m)Ti}\cdot\mathbf{r}) + F_{(m)T1-T2}\hat{z}\exp(\mathrm{j}2k_{(m)}z), \quad i = 1, 2,\\
&F_{(m)Ti} = -\mathrm{j}(\kappa + 4\mu/3 + A/2 + B)K_T^3 u_{(m)Ti}^2,\\
&F_{(m)T1-T2} = -\mathrm{j}2\{\mu + A/4 - \cos 2\theta_{(m)T}(\kappa + \mu/3 + A/4 + B)\}u_{(m)T1}u_{(m)T2}k_{(m)}K_T^2,
\end{aligned} \tag{6}$$

where $A$, $B$ (here $C$ does not appear) are third order elastic constants used by Landau and Lifshitz. It is readily seen that the direction of $\mathbf{F}(\mathbf{u}^{(1)})$ is in the $yz$ plane.

Besides $\mathbf{F}(\mathbf{u}^{(1)})$ in the interior of solid plate, there is the stress tensor of double the fundamental frequency at $y = \pm d$, denoted by $\mathbf{P}^{(2)}(\mathbf{u}^{(1)})$. Here $\mathbf{P}^{(2)}(\mathbf{u}^{(1)})$ corresponds to the quadric term of expression of the first Piola–Kirchhoff stress tensor. The three tensor components of $\mathbf{P}^{(2)}(\mathbf{u}^{(1)})$ associated with the $m$th SH mode take the following forms [12]:

$$\begin{aligned}
&P_{xy}^{(2)} = 0,\\
&P_{yy}^{(2)} = \left(\mu + \frac{A}{4}\right)\left(\frac{\partial u_x^{(1)}}{\partial y}\right)^2 + \tfrac{1}{2}(\kappa - \tfrac{2}{3}\mu + B)\left\{\left(\frac{\partial u_x^{(1)}}{\partial y}\right)^2 + \left(\frac{\partial u_x^{(1)}}{\partial z}\right)^2\right\},\\
&P_{zy}^{(2)} = \left(\mu + \frac{A}{4}\right)\frac{\partial u_x^{(1)}}{\partial y}\frac{\partial u_x^{(1)}}{\partial z}.
\end{aligned} \tag{7}$$

On basis of the boundary condition of SH mode, i.e., $\partial u_x^{(1)}/\partial y|_{y=\pm d} = 0$, there are the relations at the surfaces $y = \pm d$:

$$\begin{aligned}
&P_{xy}^{(2)}\Big|_{y=\pm d} = 0, \quad P_{zy}^{(2)}\Big|_{y=\pm d} = 0,\\
&P_{yy}^{(2)}\Big|_{y=\pm d} = 2\left(\kappa - \tfrac{2}{3}\mu + B\right)(-1)^{m+1}k_{(m)}^2 u_{(m)T1}^2\exp(\mathrm{j}2k_{(m)}z).
\end{aligned} \tag{8}$$

According to the modal analysis of waveguide excitation, the volume driving force $\mathbf{F}(\mathbf{u}^{(1)})$ and the surface stress tensor component $P_{yy}^{(2)}|_{y=\pm d}$ may be thought of as a volume source and a surface source, respectively, and the function of $\mathbf{F}(\mathbf{u}^{(1)})$ and $P_{yy}^{(2)}|_{y=\pm d}$ is to produce a series of double frequency Lamb modes (DFLMs) [2,9]. It should be noted that there is no double frequency SH mode generation since the $ox$-component of $\mathbf{F}(\mathbf{u}^{(1)})$ is zero and $P_{xy}^{(2)} = 0$. The fields of the DFLM with ordinal number $n$ are shown in Fig. 1, where the field quantities are assumed to be independent of the $x$ co-ordinate, $k_{(n)}^{(L)} = 2\omega/c_{(n)}^{(L)}$ is the $oz$-axis component of the $n$th DFLM wave vectors $\mathbf{K}_{(n)Ti}^{(L)}$ and $\mathbf{K}_{(n)Li}^{(L)}$ ($i = 1, 2$), and $c_{(n)}^{(L)}$ is the corresponding phase velocity. The total second harmonics of the $m$th SH mode can be expressed by the mode expansion of DFLMs [2,9]

$$\mathbf{U}_{(m)}^{(2\omega)}(y, z) = \sum_n a_n(z)\mathbf{u}_{(n)}^{(L)}(y), \tag{9}$$

where

$$\mathbf{u}_{(n)}^{(L)}(y) = \sum_{i=1}^{2}\left[\mathbf{u}_{(n)Ti}^{(L)} + \mathbf{u}_{(n)Li}^{(L)}\right]\exp(-\mathrm{j}k_{(n)}^{(L)}z) = \left[u_{(n)y}^{(L)}(y)\hat{y} + u_{(n)z}^{(L)}(y)\hat{z}\right] \tag{10}$$

is the field function of the $n$th DFLM, and $a_n(z)$ is the $n$th DFLM amplitude associated with $z$. The equation governing $a_n(z)$ is given by [2]

$$4P_{nn}\left(\frac{\partial}{\partial z} - \mathrm{j}k_{(n)}^{(L)}\right)a_n(z) = f_{Vn}(z) + f_{Sn}(z), \tag{11}$$

where

$$f_{Vn}(z) = \int_{-d}^{+d} \mathrm{j}2\omega\ \tilde{\mathbf{u}}_{(n)}^{(L)}(y)\cdot\mathbf{F}(\mathbf{u}^{(1)})\,\mathrm{d}y \tag{12}$$

and

$$f_{Sn}(z) = \mathrm{j}2\omega\tilde{\mathbf{u}}_{(n)}^{(L)}\cdot\mathbf{P}^{(2)}(\mathbf{u}^{(1)})\cdot\hat{y}\Big|_{y=-d}^{y=+d} = \mathrm{j}2\omega\ \tilde{u}_{(n)y}^{(L)}\ P_{yy}^{(2)}\Big|_{y=-d}^{y=+d} \tag{13}$$

are the excitation functions due to both volume source $\mathbf{F}(\mathbf{u}^{(1)})$ and surface stress tensor component $P_{yy}^{(2)}|_{y=\pm d}$, and $P_{nn}$ is the average power flow per unit width along the $x$-axis for the $n$th DFLM

$$\begin{aligned} P_{nn} &= \mathrm{Re}\int_{-d}^{+d}\left[-\frac{1}{2}\frac{\tilde{\partial}}{\partial t}\mathbf{u}_{(n)}(y)\cdot\mathbf{T}_n\cdot\hat{z}\right]\mathrm{d}y \\ &= \mathrm{Re}\int_{-d}^{+d}(-\mathrm{j}\omega)\left[\tilde{u}_{(n)y}^{(L)}(y)\,T_{(n)yz}(y) + \tilde{u}_{(n)z}^{(L)}(y)\,T_{(n)zz}(y)\right]\mathrm{d}y. \end{aligned} \tag{14}$$

In Eqs. (12)–(14) and below, a variable with '~' means the complex conjugate of the corresponding variable. $\mathbf{T}_n$ is the stress tensor concerned with the $n$th DFLM, and its components, $T_{(n)yz}$ and $T_{(n)zz}$ are presented in Appendix A. Further the expression of $a_n(z)$ is found to be

$$a_n(z) = a_n'\int_0^z d^{-1}\exp[\mathrm{j}(2k_{(m)} - k_{(n)}^{(L)})\xi]\,\mathrm{d}\xi\exp[\mathrm{j}k_{(n)}^{(L)}z] \tag{15}$$

and

$$\begin{aligned} a_n' &= \frac{[f_{Vn}(z) + f_{Sn}(z)]\exp(-\mathrm{j}2k_{(m)}z)}{4P_{nn}}\,d \\ &= \frac{\exp(-\mathrm{j}2k_{(m)}z)}{4P_{nn}}\,d\left\{\int_{-d}^{+d}\mathrm{j}2\omega\ [\tilde{u}_{(n)y}^{(L)}(y)\ F_{(m)y}(y) + \tilde{u}_{(n)z}^{(L)}(y)\ F_{(m)z}(y)]\,\mathrm{d}y\right. \\ &\qquad \left. + \mathrm{j}2\omega\ \tilde{u}_{(n)y}^{(L)}\ P_{yy}^{(2)}\Big|_{y=-d}^{y=+d}\right\}, \end{aligned} \tag{16}$$

where $F_{(m)y}(y)$ and $F_{(m)z}(y)$ are the $oy$ and $oz$ components of $\mathbf{F}(\mathbf{u}^{(1)})$ [neglecting the factor $\exp(\mathrm{j}2k_{(m)}z)$]. Further analysis indicates that the scale of $a_n'$ is $u_{(m)T1}^2 d^{-1}$. The integral in the right-hand side of Eq. (15) is readily found to be

$$\int_0^z d^{-1}\exp[\mathrm{j}2k_{(m)}\xi - \mathrm{j}k_{(n)}^{(L)}\xi]\,\mathrm{d}\xi = \frac{\sin[k_{(m)} - k_{(n)}^{(L)}/2]z}{[k_{(m)} - k_{(n)}^{(L)}/2]d}\exp[\mathrm{j}k_{(m)} - \mathrm{j}k_{(n)}^{(L)}/2]z. \tag{17}$$

From Eqs. (15) and (17) it is easy to find that $a_n(z)$ is linearly proportional to propagation distance $z$ once the condition $k_{(m)} = k_{(n)}^{(L)}/2$ (i.e., $c_{(m)} = c_{(n)}^{(L)}$) is satisfied. It is also found that there is a cumulative growth effect as $c_{(m)} \approx c_{(n)}^{(L)}$ where the magnitude of $a_n(z)$ accumulates with $z$ as the form of sine function within the first quadrant. When the $m$th SH mode propagation arrives at

$$z_{(n)} = \frac{c_{(n)}^{(L)} c_{(m)} d}{4fd(c_{(n)}^{(L)} - c_{(m)})} \tag{18}$$

there is maximum of the magnitude of $a_n(z)$. After that the magnitude of $a_n(z)$ starts to decrease. The value of $z_{(n)}$ can be used to characterize the degree of cumulative growth effect of the $n$th DFLM component. As an example, $z_{(n)} = \infty$ (i.e., $c_{(m)} = c_{(n)}^{(L)}$) means the case in which there is a complete phase match for the $n$th DFLM generated by excitation functions $f_{Vn}(z)$ and $f_{Sn}(z)$ in different position (denoted by $z$). In a word the contribution of the $n$th DFLM component to $\mathbf{U}_{(m)}^{(2\omega)}(y, z)$ is determined by the difference between $c_{(m)}$ and $c_{(n)}^{(L)}$.

From Eqs. (15) and (17) it is easy to find that $a_{(n)}(z) = 0$ as $z = 0$, which means that the initial condition of harmonic generation is satisfied for the $n$th component of DFLMs. Note that, in the present analysis, only the propagation modes of DFLMs is considered and the evanescent modes are neglected. The influence of evanescent modes can be negligible after some propagation distance. Propagation modes play a dominant role.

For the $n$th DFLM there are the relationships:

$$\begin{aligned} &u_{(n)y}^{(L)}(y) = -u_{(n)y}^{(L)}(-y), \quad u_{(n)z}^{(L)}(y) = u_{(n)z}^{(L)}(-y), \quad \text{symmetric case,} \\ &u_{(n)y}^{(L)}(y) = +u_{(n)y}^{(L)}(-y), \quad u_{(n)z}^{(L)}(y) = -u_{(n)z}^{(L)}(-y), \quad \text{antisymmetric case.} \end{aligned} \tag{19}$$

From the form of $\mathbf{F}(\mathbf{u}^{(1)})$ there are

$$F_{(m)y}(y) = -F_{(m)y}(-y), \quad F_{(m)z}(y) = F_{(m)z}(-y). \tag{20}$$

Combining Eqs. (8), (16), (19) and (20) yields

$$\begin{aligned} a_n' &= 0, \quad \text{antisymmetric case,} \\ a_n' &\neq 0, \quad \text{symmetric case,} \end{aligned} \tag{21}$$

which means that only the symmetric DFLMs occur accompanying the $m$th SH mode propagation. So the field of the total second harmonics $\mathbf{U}_{(m)}^{(2\omega)}(y, z)$ consisting of a series of DFLMs is symmetrical.

As described above, the modal analysis technique of waveguide excitation is successfully applied in analyzing second-harmonic generation of a single SH mode. There are body forcing and surface stress tensor functions due to the elastic non-linearity of plate material as a SH mode propagates in the plate. Second order volume forcing and surface stress tensor functions give rise to generation of a series of DFLMs. The contribution of each DFLM is associated with the difference of phase velocities of SH mode and the DFLM. The degree of cumulative growth effect of DFLM component can be characterized by $z_{(n)}$. Under the prerequisite of second order perturbation, all analyses are exact. Obviously, the present analysis technique of second-harmonic generation overcomes the previous problems of indeterminacy of the non-cumulative harmonic terms [7].

## 3. Computation analyses

To understand the above analysis results, we perform a computational analysis. The material of elastic plate is assumed to be aluminium. The corresponding physical parameters are: $\rho = 2700\,\mathrm{kg/m^3}$, $\kappa = 74\,\mathrm{GPa}$, $\mu = 26\,\mathrm{GPa}$, $A = -100\,\mathrm{GPa}$, $B = -600\,\mathrm{GPa}$ [13]. Fig. 2 shows the dispersion curves of SH modes and symmetric DFLMs (because only symmetric DFLMs occur). The dispersion curves of SH modes are calculated by Eq. (5), and the dispersion curves of the symmetric DFLMs are computed by the dispersion relation of symmetric Lamb modes using $2f$ instead of $f$ [2]. In Fig. 2 the intersections of two sets of dispersion curves satisfy $c_{(m)} = c^{(L)}_{(n)}$.

In order to determine $a_n(z)$, $a'_n$ must be computed first. Fig. 3 gives the curves of $a'_n$ for $S_2$, $S_3$, and $S_4$ DFLMs, where the ordinal number of SH mode is 3. The value of $a_n(z)$ can be determined after $a'_n$ is given. In Fig. 3(d) there are intersections between the beeline $L$ and the dispersion curves [there is $c_{(3)} = c^{(L)}_{(3)}$ at intersection $P$]. The physical parameters of these intersections corresponding to the different DFLMs are listed in Table 1.

Generally, the measurement of the second-harmonic fields is performed on the plate surface. Fig. 4 presents the amplitudes of $a_n(z)\mathbf{u}^{(L)}_{(n)}(y)$ (see Eq. (9)) for $S_2$, $S_3$, and $S_4$ DFLMs on the plate surface. The results show that $S_3$ DFLM amplitudes accumulate with propagation distance $z$ as $c_{(3)} = c^{(L)}_{(3)}$, and that the displacement amplitudes of $S_2$ and $S_4$ DFLMs oscillate greatly as there is an obvious difference between $c_{(3)}$ and $c^{(L)}_{(n)}$ ($n = 2$, 4, $z_{(n)}$ is small). From Fig. 4 it is obvious that the contribution of $S_2$ and $S_4$ DFLMs to $\mathbf{U}^{(2\omega)}_{(m)}(y,z)$ is much smaller than that of $S_3$ after the third SH mode propagate some distance. In this case the contribution of $S_2$ or $S_4$ DFLMs to $\mathbf{U}^{(2\omega)}_{(m)}(y,z)$ may be neglected.

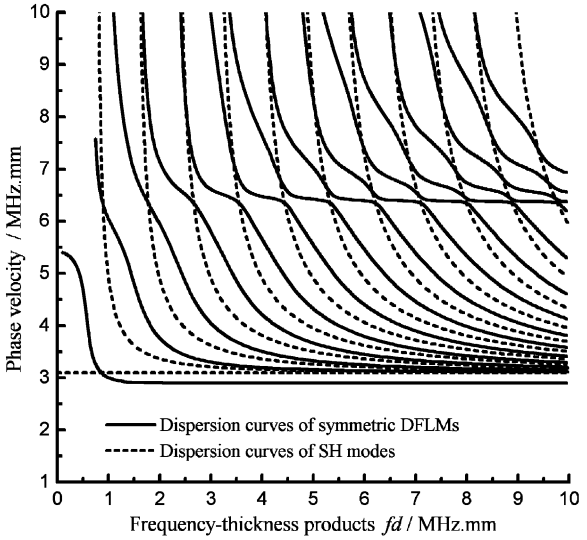


Fig. 2. Dispersion curves of SH and symmetric DFLM modes.

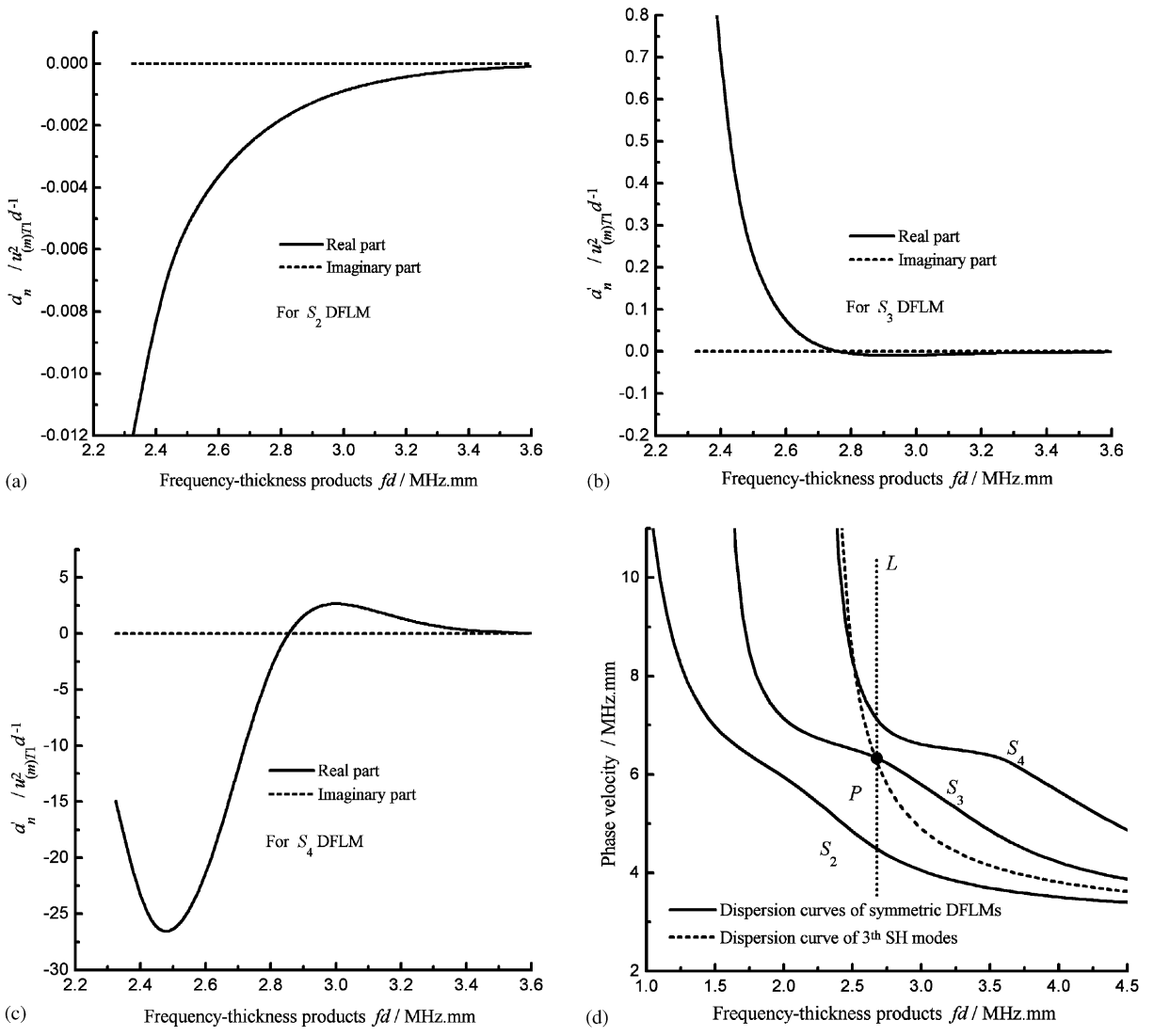


Fig. 3. The curves of $a'_n$ versus $fd$ for some DFLMs, the ordinal number of SH mode is 3: (a) for $S_2$ DFLM; (b) for $S_3$ DFLM; (c) for $S_4$ DFLM; (d) dispersion curves in the near region of intersection $P$.

Table 1
Some parameters concerned with the intersections in Fig. 3(d)

| | $fd$ (MHz mm) | $c_{(3)}$ or $c_{(n)}^{(L)}$ (MHz mm) | $a'_n/u^2_{(m)T1}\,d^{-1}$ |
|---|---|---|---|
| Third SH mode | 2.664 | 6.350 | — |
| $S_2$ DFLM | 2.664 | 4.483 | $(-2.88\times10^{-3}, 0)$ |
| $S_3$ DFLM | 2.664 | 6.350 | $(2.89\times10^{-2}, 0)$ |
| $S_4$ DFLM | 2.664 | 7.184 | $(-15.63, 0)$ |

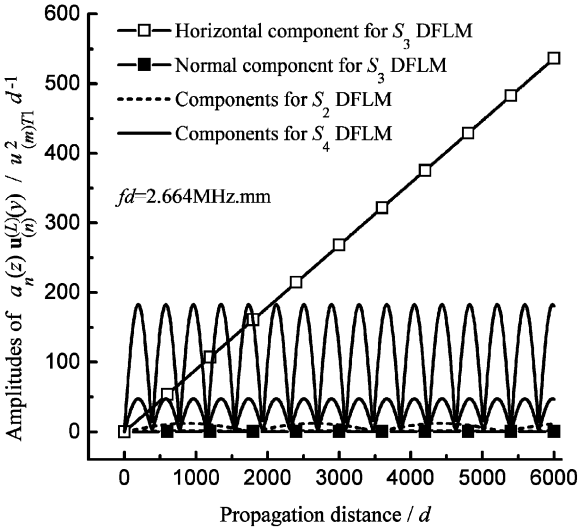


Fig. 4. Amplitudes of $a_n(z)\mathbf{u}_{(n)}^{(L)}(y)$ for some DFLMs.

## 4. Conclusions

By using modal analysis, the exact solution to the second harmonics of a SH mode was successfully derived under second order perturbation. The second-harmonic fields of a SH mode can be expanded as a series of DFLMs. The contribution of each DFLM component to second-harmonic fields of a SH mode is dependent of the difference of phase velocities of the SH mode and the corresponding DFLM. The DFLM field component has a cumulative growth effect as its phase velocity exactly or approximately equals that of SH mode. On the other hand, its contribution to the total second harmonics may be neglected if the phase velocity of SH mode is quite different from that of the DFLM component. It is found that only the symmetric DFLM component can be generated. Therefore, the field of second-harmonic generation of a SH mode is symmetrical. This work presents an exact analysis approach for investigating the problems of generation of the second harmonics of guided wave modes.

## Acknowledgements

This work was supported by National Natural Science Foundation of China (10004016).

## Appendix A

The components of $\mathbf{u}_{(n)}^{(L)}(y)$, i.e., $u_{(n)y}^{(L)}(y)$ and $u_{(n)z}^{(L)}(y)$, are given by

$$u_{(n)y}^{(L)}(y) = \Big\{\cos\theta_{(n)L}^{(L)} \exp\Big[+\mathrm{j}\alpha_{(n)L}^{(L)} k_{(n)}^{(L)} y\Big] - B_{(n)1} \sin\theta_{(n)T}^{(L)} \exp\Big[+\mathrm{j}\alpha_{(n)T}^{(L)} k_{(n)}^{(L)} y\Big]$$
$$-B_{(n)2} \cos\theta_{(n)L}^{(L)} \exp\Big[-\mathrm{j}\alpha_{(n)L}^{(L)} k_{(n)}^{(L)} y\Big] + B_{(n)3} \sin\theta_{(n)T}^{(L)} \exp\Big[-\mathrm{j}\alpha_{(n)T}^{(L)} k_{(n)}^{(L)} y\Big]\Big\},$$

$$u_{(n)z}^{(L)}(y) = \left\{ \sin\theta_{(n)L}^{(L)} \exp\left[+\mathrm{j}\alpha_{(n)L}^{(L)} k_{(n)}^{(L)} y\right] + B_{(n)1} \cos\theta_{(n)T}^{(L)} \exp\left[+\mathrm{j}\alpha_{(n)T}^{(L)} k_{(n)}^{(L)} y\right] \right.$$
$$\left. + B_{(n)2} \sin\theta_{(n)L}^{(L)} \exp\left[-\mathrm{j}\alpha_{(n)L}^{(L)} k_{(n)}^{(L)} y\right] + B_{(n)3} \cos\theta_{(n)T}^{(L)} \exp\left[-\mathrm{j}\alpha_{(n)T}^{(L)} k_{(n)}^{(L)} y\right] \right\},$$

with

$$\left|\mathbf{K}_{(n)Q1}^{(L)}\right| = \left|\mathbf{K}_{(n)Q2}^{(L)}\right| = K_Q^{(L)} = 2\omega/c_Q, \quad k_{(n)}^{(L)} = K_Q^{(L)} \sin\theta_{(n)Q}^{(L)}, \quad \cos\theta_{(n)Q}^{(L)} = \alpha_{(n)Q}^{(L)} \sin\theta_{(n)Q}^{(L)},$$
$$\alpha_{(n)Q}^{(L)} = \sqrt{\left[c_{(n)}^{(L)}/c_Q\right]^2 - 1}, \quad Q = T, L,$$

where $u_{(n)L1}^{(L)} = 1$, $B_{(n)1} = u_{(n)T1}^{(L)}/u_{(n)L1}^{(L)}$, $B_{(n)2} = u_{(n)L2}^{(L)}/u_{(n)L1}^{(L)}$, and $B_{(n)3} = u_{(n)T2}^{(L)}/u_{(n)L1}^{(L)}$; $u_{(n)Li}^{(L)}$ and $u_{(n)Ti}^{(L)}$ ($i = 1, 2$) are the amplitudes of $\mathbf{u}_{(n)Li}^{(L)}$ and $\mathbf{u}_{(n)Ti}^{(L)}$; $B_{(n)1}$, $B_{(n)2}$ and $B_{(n)3}$ can be determined after the $n$th DFLM is given; $Q = L$ or $T$ means that the corresponding physical quantity is associate with longitudinal or transverse wave. There are relations: $B_{(n)2} = \pm 1$, and $B_{(n)1} = \pm B_{(n)3}$. Here '+' and '−' correspond to the symmetric and antisymmetric cases, respectively.

The components of $\mathbf{T}_n$ are

$$T_{(n)yz}(y) = \mathrm{j}k_{(n)}^{(L)} \left\{ M_1 \exp\left[+\mathrm{j}\alpha_{(n)L}^{(L)} k_{(n)}^{(L)} y\right] + B_{(n)1} M_2 \exp\left[+\mathrm{j}\alpha_{(n)T}^{(L)} k_{(n)}^{(L)} y\right] \right.$$
$$\left. - B_{(n)2} M_1 \exp\left[-\mathrm{j}\alpha_{(n)L}^{(L)} k_{(n)}^{(L)} y\right] - B_{(n)3} M_2 \exp\left[-\mathrm{j}\alpha_{(n)T}^{(L)} k_{(n)}^{(L)} y\right] \right\},$$

$$T_{(n)zz}(y) = \mathrm{j}k_{(n)}^{(L)} \left\{ M_3 \exp[+\mathrm{j}\alpha_{(n)L}^{(L)} k_{(n)}^{(L)} y] + B_{(n)1} M_4 \exp[+\mathrm{j}\alpha_{(n)T}^{(L)} k_{(n)}^{(L)} y] \right.$$
$$\left. + B_{(n)2} M_3 \exp[-\mathrm{j}\alpha_{(n)L}^{(L)} k_{(n)}^{(L)} y] + B_{(n)3} M_4 \exp[-\mathrm{j}\alpha_{(n)T}^{(L)} k_{(n)}^{(L)} y] \right\},$$

where $M_1 = 2\mu \cos\theta_{(n)L}^{(L)}$, $M_2 = \mu \sin\theta_{(n)T}^{(L)} [\alpha_{(n)T}^{(L)2} - 1]$, $M_3 = \alpha_{(n)L}^{(L)} \cos\theta_{(n)L}^{(L)} [\kappa - 2\mu/3] + \sin\theta_{(n)L}^{(L)} [\kappa + 4\mu/3]$, and $M_4 = 2\mu \cos\theta_{(n)T}^{(L)}$.

## References


[1] L.M. Brekhovskikh, Waves in Layered Media, Academic Press, New York, 1960.

[2] B.A. Auld, Acoustic Fields and Waves in Solids, Wiley, New York, 1973.

[3] D.C. Price, B.J. Martin, D.A. Scott, Ultrasonic guided waves for inspection of bonded panels, Acoustics Australia 27 (1999) 95–101.

[4] J.H. Ginsberg, K.T. Shu, The role of nonlinearities in propagation, reflection, and transmission of stress waves and possible application to NDE, Review of Progress in Quantitative NDE 10B (1991) 1829–1836.

[5] Yongping Zheng, G.M.Roman, I.Y. Solodov, Nonlinear acoustic applications for material characterization: a review, Canadian Journal of Physics 77 (1999) 927–967.

[6] M.F. Hamliton, D.T. Blackstock, Nonlinear Acoustics, Academic, New York, 1998.

[7] M.X. Deng, Cumulative second-harmonic generation accompanying nonlinear shear horizontal mode propagation in a solid plate, Journal of Applied Physics 84 (1998) 3500–3505.

[8] S. Zhou, Y. Shui, Nonlinear reflection of bulk acoustic waves at an interface, Journal of Applied Physics 72 (1992) 5070–5080.

[9] X. Jia, Modal analysis of Lamb mode wave generation in elastic plates by liquid wedge transducers, Journal of the Acoustical Society of America 101 (1997) 834–842.

[10] I. Nunez, R.K. Ing, C. Negreira, M. Fink, Transfer and Green functions based on modal analysis for Lamb waves generation, Journal of the Acoustical Society of America 107 (2000) 2370–2378.
[11] G.S. Kino, Acoustic Waves: Devices, Imaging, and Analog Signal Processing, Prentice-Hall, Englewood Cliffs, NJ, 1987.
[12] G.L. Jone, D.R. Kobett, Interaction of elastic waves in an isotropic solid, Journal of the Acoustical Society of America 35 (1963) 5–12 and references therein.
[13] R.F.S. Hearmon, Landolt–Börnstein, Numerical Data and Functional Relationship in Science and Technology, Group III, Vol. 11, Springer, New York, 1979.